

# Linking the Chemical and Physical Effects of CO<sub>2</sub> Injection to Geophysical Parameters

## Investigators:

### *Stanford University:*

Gary Mavko, Professor (Research), Geophysics; Sally Benson, Professor (Research) Energy Resources Engineering; Tiziana Vanorio, Sr. Research Scientist, Geophysics; Stephanie Vialle, Post-Doc, Geophysics.

### *Rice University:*

Andreas Luttge, Professor, Earth Science; Rolf Arvidson, Sr. Research Scientist, Earth Science

## Abstract

This project aims to demonstrate techniques for quantitatively predicting the combined seismic signatures of CO<sub>2</sub> saturation, chemical changes to the rock frame, and pore pressure. This will be accomplished (i) by providing a better understanding the reaction kinetics of CO<sub>2</sub>-bearing reactive fluids with rock-forming minerals, and (ii) by quantifying how the resulting long-term, CO<sub>2</sub>-injection-induced changes to *the rock pore space and frame* (e.g. porosity, permeability, mineral dissolution, and cementation) *affect seismic parameters in the reservoir*.

This research involves laboratory, theoretical, and computational tasks in the fields of both Rock Physics and Geochemistry. Samples have been selected based on mineralogy (carbonates, sandstones, and calcite-cemented sandstones), porosity, pore and cement type. Ultrasonic P- and S-wave velocities are being measured over a range of confining pressures while injecting CO<sub>2</sub> and brine into the samples. Pore fluid pressure will be varied and monitored together with porosity during injection. The measurement of rock physics properties will be integrated and complemented by those obtained via geochemical experiments to link the physical (e.g. porosity enhancement, selective dissolution and change in microstructure) and chemical processes (e.g. reaction type and dissolution rates) underlying the mechanisms triggered by CO<sub>2</sub> injection. We will also develop computational and analysis tools needed to simulate multi-fluid flow at the pore scale while including dissolution effects.

Experiments to date on carbonate samples show that both P - and S- wave velocities under dry and saturated conditions decrease over time, due to dissolution during injection of CO<sub>2</sub>-bearing brine. However, for similar injected volumes of fluid, the magnitude of these changes differs from one sample to another. It appears that the different responses of the rocks to CO<sub>2</sub> injection are related, in part, to their initial microstructures. Samples with loosely-fitting micritic grains have a larger sensitivity to CO<sub>2</sub> injection than the samples with more tighter-fitting “mosaic” grains. The decrease in the velocities with

CO<sub>2</sub> injection is due to permanent and irreversible changes in the microstructure, as documented by the time-lapse SEM monitoring. SEM images show a) porosity enhancement, b) changes in the texture with formation of features similar to oblitative diagenetic structure caused by recrystallization and/or replacement and c) oil expelled from the pore system during the injection. Porosity enhancement has been quantified and monitored while performing the injections experiments. It has been found that this is the result of two competing and interdependent mechanisms: chemical dissolution of the mineral composing the rock causing a porosity *increase* and weakening of the rock frame and the subsequent mechanical compaction of the rock under the effect of pressure, causing a small porosity *decrease*. Samples containing residual oil (as would be the case for sequestration in a depleted reservoir) show that the injection of CO<sub>2</sub>-rich fluids causes oil to be expelled from the pores.

Our estimates of reactive surface area are two orders of magnitude smaller than the geometrical surface area obtained by erosion-dilatation. This means that the surface areas measured (by gas adsorption like BET, by vertical scanning interferometry, atomic force microscopy, laser confocal microscopy or X-rays tomography) or geometrically constructed are not relevant for the reactivity of the rock. Work has begun on developing tools for numerical simulation of reactive flow in the rock pore space, as a means to better understand and to predict changes of the type observed in the lab.

The subcontract to Rice University was finally put into place this spring, and will be performed by Prof. Andreas Lutge and Dr. Rolf Arvidson. Analysis of reaction rate during crystal growth, dissolution, oxidation, hydration, etc. will be made by them by using Vertical-Scanning-Microscopy (VSM) that allows imaging of the dissolution process at the molecular scale. In particular, the analysis will be made through comparison of VSI digital height maps of surface topography as a function of time. Results will provide the requisite data for modeling the acoustic response of dissolution. Flow-through experiments on rock plugs upon measurements of the acoustic properties along with CT-scan imaging will be made to quantify and image changes to the host rock pore structure and permeability due to dissolution and precipitation reactions.

### **Introduction:**

Monitoring, verification, and accounting (MVA) of CO<sub>2</sub> fate are three fundamental needs in geological sequestration. The primary objective of MVA protocols is to identify and quantify (1) the injected CO<sub>2</sub> stream within the injection/storage horizon and (2) any leakage of sequestered gas from the injection horizon, providing public assurance. Thus, the success of MVA protocols based on seismic prospecting depends on having robust methodologies for *detecting* the amount of change in the elastic rock property, *assessing* the *repeatability* of measured changes, and *interpreting and analyzing* the detected changes to make quantitative predictions of the movement, presence, and permanence of CO<sub>2</sub> storage, including leakage from the intended storage location. This project addresses the problem of how to interpret and analyze the detected seismic changes so that quantitative predictions of CO<sub>2</sub> movement and saturation can be made. The main goals are:

- (a) linking the chemical and the physical changes occurring in the rock samples upon injection;
- (b) assessing the type and magnitude of reductions caused by rock-fluid interactions at the grain/pore scale;
- (c) providing the basis for CO<sub>2</sub>-optimized physical-chemical models involving frame substitution schemes.

### **Background:**

Having the appropriate rock-physics model is generally a key element for time-lapse seismic monitoring of the subsurface, both to infer the significance of detectable changes (*i.e.* qualitative interpretation) and to convert them into actual properties of the reservoir rocks (*i.e.* quantitative interpretation). Nevertheless, because of the peculiar ability of CO<sub>2</sub>-rich water to promote physicochemical imbalances within the rock, we must address whether traditional rock-physics models can be used to invert the changes in geophysical measurements induced in porous reservoirs by the injection of CO<sub>2</sub>, making it possible to ascribe such changes to the presence or upward migration of CO<sub>2</sub> plumes. Making this determination requires an understanding of the seismic response of CO<sub>2</sub>-water-rock systems. Seismic reservoir monitoring has traditionally treated the changes in the reservoir rock as a physical-mechanical problem—that is, changes in seismic signatures are mostly modeled as functions of saturation and stress variations (*e.g.* pore and overburden pressure) and/or intrinsic rock properties (*e.g.* mineralogy, clay content, cementation, diagenesis...). Specifically, modeling of fluid effects on seismic data has been based almost exclusively on Gassmann's equations, which describe the interaction of fluid compressibility with the elastic rock frame to determine the overall elastic behavior of rock. Beginning with the bulk ( $K_s$ ) and shear ( $\mu_s$ ) moduli of the mineral composing the rock, we use Gassmann's fluid substitution scheme to compute the bulk modulus of the saturated rock ( $K_{sat}$ ) from the bulk modulus of the fluid ( $K_{fl}$ ) and from that of dry rock ( $K_{dry}$ ). However, depending on the properties of the mineral composing the rock and the properties of the fluid, complex rock-fluid interactions may occur at the pore scale, leading to dissolution and formation of new mineralogical phases. All these physical modifications may compete in changing macroscopic rock properties such as permeability, porosity, and elastic velocities, which, in turn, can change the baseline properties for the Gassmann's fluid substitution scheme. This entails two consequences: (a) a classical fluid-substitution scheme may underpredict time-lapse changes and thus mislead 4D monitoring studies; and (b) predictions of *in situ* velocity will compensate for the chemically softened velocities with erroneous estimates of saturations and/or pore pressure.

### **Results**

#### **Laboratory measurements on carbonate rocks (core plugs) during injection of CO<sub>2</sub>-rich water**

The results to date have involved continuation of monitoring the changes in ultrasonic P- and S-wave velocities and transport properties of rocks associated with chemical interactions between minerals and pore fluids, namely dissolution/precipitation reactions induced by CO<sub>2</sub>-rich water injection. Details of the experimental device and methodology

were given in our previous yearly Progress Report, dated April, 2010. Briefly, the experiment consists of continuously injecting CO<sub>2</sub>-rich water (pH about 3.2) into carbonate core plugs, stopping regularly to measure P- and S-wave velocities and sample length, both under fully saturated conditions and dry conditions (achieved by blowing dry helium directly in the pressure vessel). We are also performing measurements of the geochemical properties (i.e., pH and Calcium content) of the CO<sub>2</sub>-rich fluids and their evolution upon injection, as well as time-lapse SEM imaging to monitor and quantify the changes in the rock microstructure.

In this report, we present the changes in P- and S- wave velocities (Figure 1), transport properties and the associated changes in the rock microstructure (Figures 2, 3 and 4) in carbonate rocks having different initial microstructures. Table 1 summarizes measured total changes in acoustic, hydraulic and rock properties that occurred during injection.

Table 1: Table summarizing the acoustic, hydraulic and rock properties before and after injection of CO<sub>2</sub>-rich water.

Sample ID	Injected Volumes*	Before Injection				After Injection			
		Φ (%)	k (mD)	Vp (m/s)	Vs (m/s)	Φ (%)	k (mD)	Vp (m/s)	Vs (m/s)
RU7855B	2078	26.3	10.3	4116	2248	27.9	>4000	3927	2104
DK34A	698	32.5	40.1	3063	1984	35.3	417	2656	1792
K86B	703	20.0	5.6	4932	2628	20.9	296	4800	?

Φ=porosity; k=permeability; Vp=P-wave velocity; Vs=S-wave velocity.

Results can be summarized as follows:

1. Figure 1 shows the variation of the dry and fluid-saturated ultrasonic P- and S-wave velocities for three carbonates as a function of injected volumes of fluid. Velocities are normalized to their pre-injection values. Injection also caused release of residual oil (observed as surface stains) that was previously trapped in the pore space. Both P - and S- wave velocities under dry and saturated conditions decrease over time for all measured samples. However, for similar injected volumes of fluid, the magnitude of these changes differs from one sample to another.
2. It appears that the different responses of the rocks to CO<sub>2</sub> injection are related, in part, to their initial microstructures. Figures 2, 3, and 4 (left panels) show SEM images of the three samples presented in Figure 1. The DK sample, a mudstone with a high amount of subhedral to euhedral, rounded-edged micritic grains, shows a higher decrease in the velocities than the two other samples, RU and K, which have tighter microstructures with interlocked grains. RU is a wackestone with both anhedral to subhedral micritic zones and a dense cement of interlocked and welded grains. K is a

packstone with few euhedral, subhedral, sometimes anhedral micritic zones and a high amount of dense and compact, sometimes coalescent cement.

3. The decrease in the velocities during CO<sub>2</sub> injection is due to permanent and irreversible changes in the microstructure, as documented by the time-lapse SEM monitoring. Images in Figures 2, 3 and 4 compare the same sites of the rock surface before and after the injection experiments. They show a) porosity enhancement, b) changes in the texture with formation of features similar to oblitative diagenetic structure caused by recrystallization and/or replacement and c) oil expelled from the pore system during the injection.
4. Porosity enhancement has been quantified and monitored while performing the injections experiments. It has been found that this is the result of two competing and interdependent mechanisms: chemical dissolution of the mineral composing the rock causing a porosity *increase* and weakening of the rock frame and the subsequent mechanical compaction of the rock under the effect of pressure, causing a small porosity *decrease*. Calculation of porosity change due to chemical dissolution was done using calcium concentrations measured in the output fluid and mass balances; calculation of porosity change due to mechanical compaction was done by using the change in the sample volume obtained by three linear potentiometers mounted in the pressure vessel. Figure 5 shows results of the calculation of total porosity for the three samples as a function of the injected pore volumes. In agreement with the different magnitudes of changes in the P- and S- wave velocities, the magnitude of porosity enhancement differs among the samples.

We can see in Figures 2, 3 and 4 that the injection of CO<sub>2</sub>-rich fluids causes oil to be expelled from the pores, as is already well known since CO<sub>2</sub> injection has been used for the past 35 years in EOR. Experiments are underway to investigate in more detail how the presence of oil in the samples affects the reactivity of the rocks and consequently their geophysical responses to CO<sub>2</sub> injection.

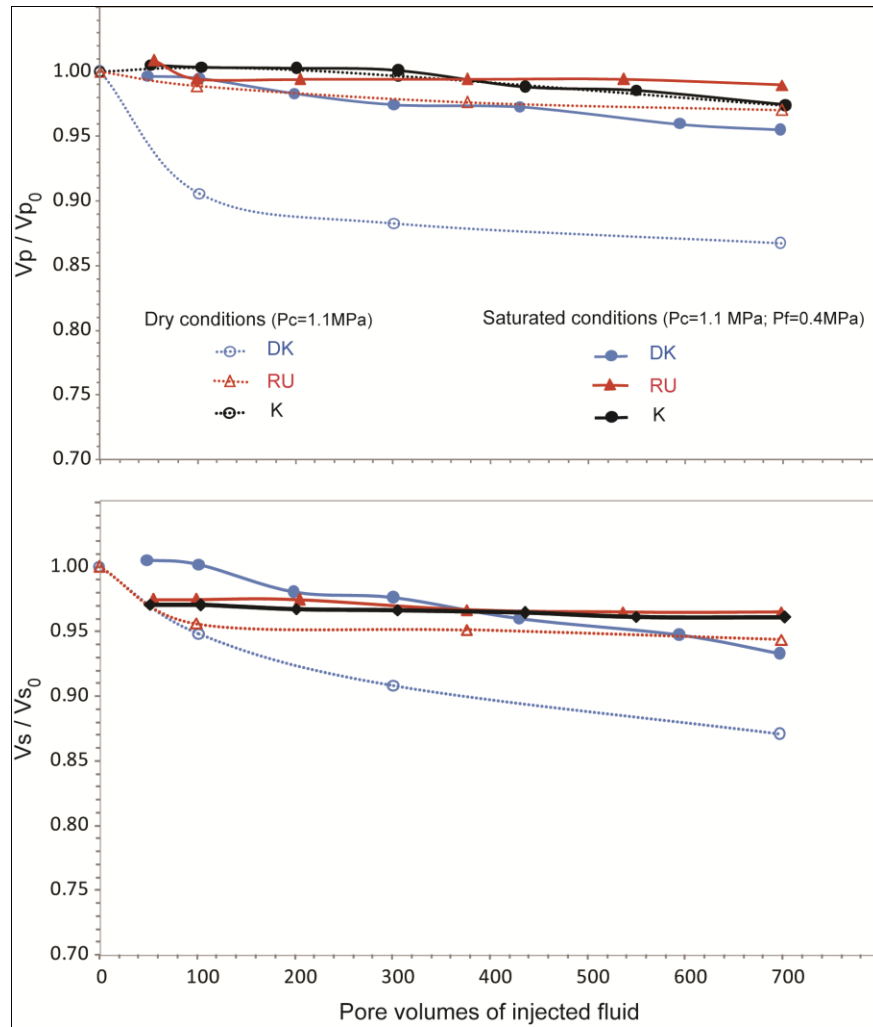


Figure 1: Ultrasonic  $V_P$  (top panel) and  $V_S$  (bottom panel) versus the injected volume of  $\text{CO}_2$ -rich water in carbonate samples. Both P- and S-velocity values are normalized with respect to their pre-injection values. Open and solid symbols represent measurements performed under dry and fully saturated conditions, respectively. Although both saturated and dry P- and S-wave velocities decrease for all measured samples, the magnitude differs depending on the rock type.

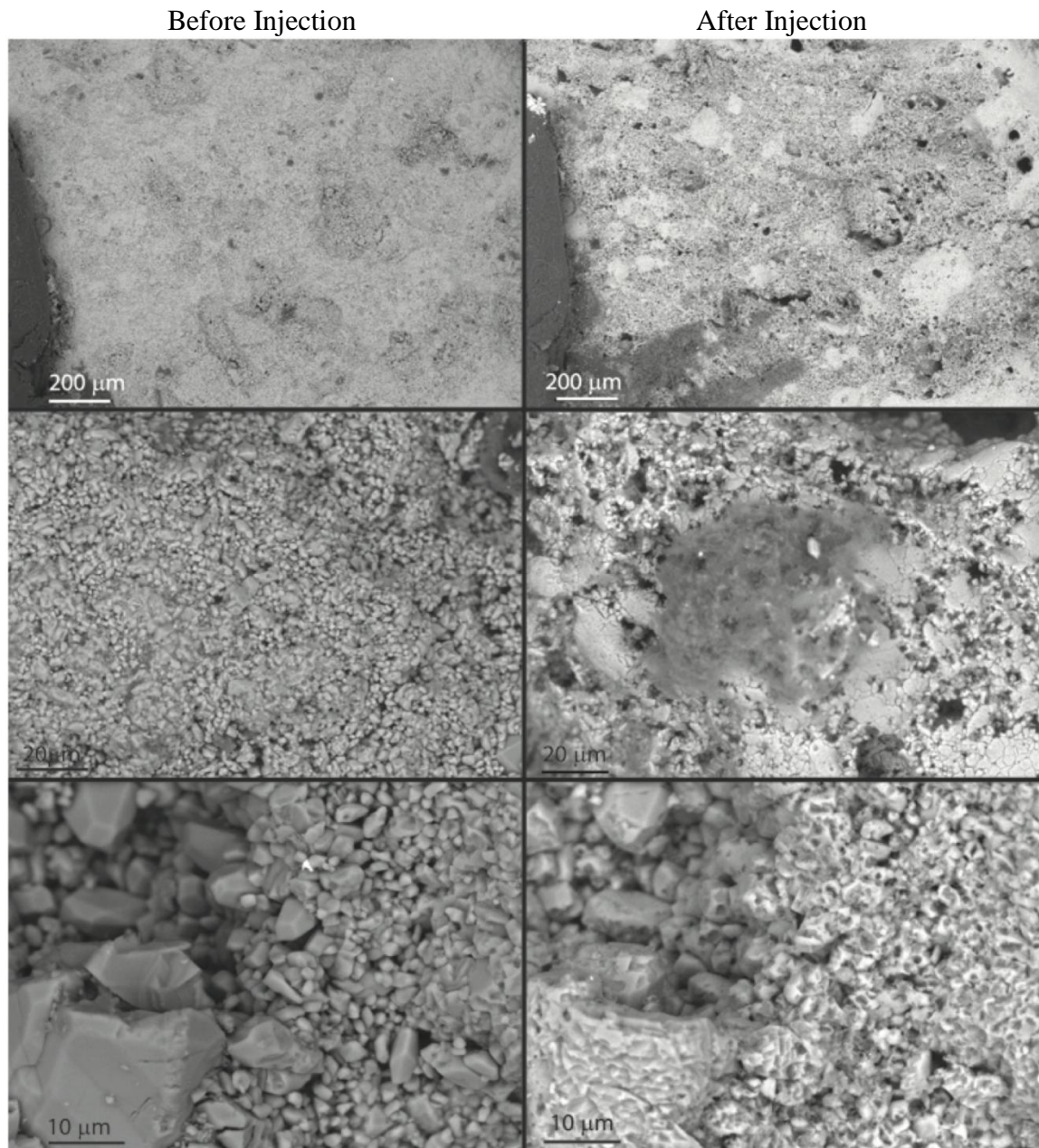


Figure 2: Time-lapse SEM images monitoring the changes in microstructure upon injection of a CO<sub>2</sub>-rich fluid in sample DK. Initial microstructure at different magnifications is shown in the left panels, and the same spots imaged after dissolution are shown in the right panels. DK is a mudstone (Dunham's classification) with a high amount of subhedral to euhedral, rounded-edged micritic grains. In some areas, microstructure can become more compact, with contacts between the grains serrate to coalescent. Heterogeneously, macropores are also present.

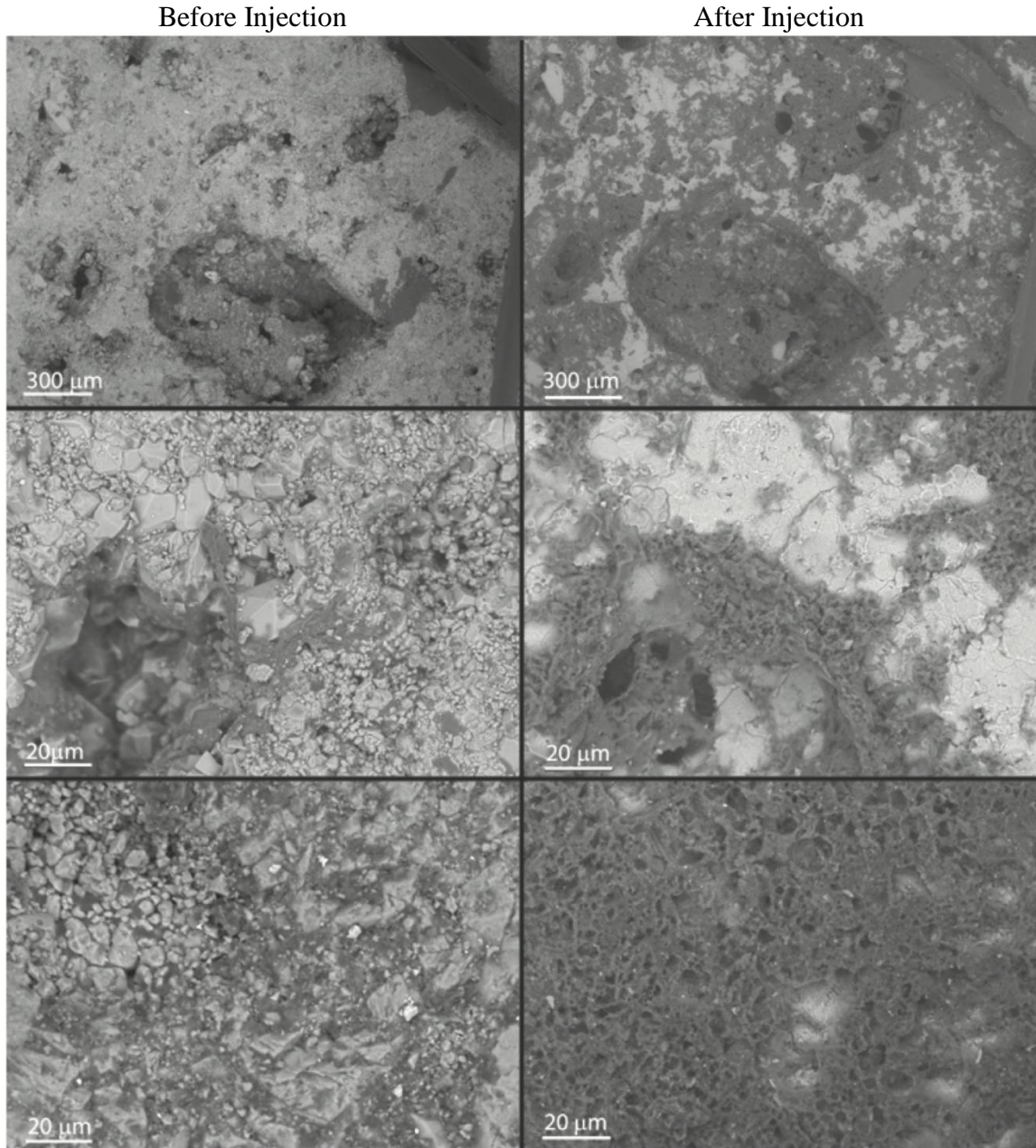


Figure 3: Time-lapse SEM images monitoring the changes in microstructure upon injection of a CO<sub>2</sub>-rich fluid in sample RU. Initial microstructure at different magnifications is shown in the left panels, and the same spots imaged after dissolution are shown in the right panels. RU is a wackestone (Dunham's classification) with both anhedral to subhedral micritic zones and a dense cement of interlocked and welded grains. Oil initially trapped in the pore space is visible in darker hue.

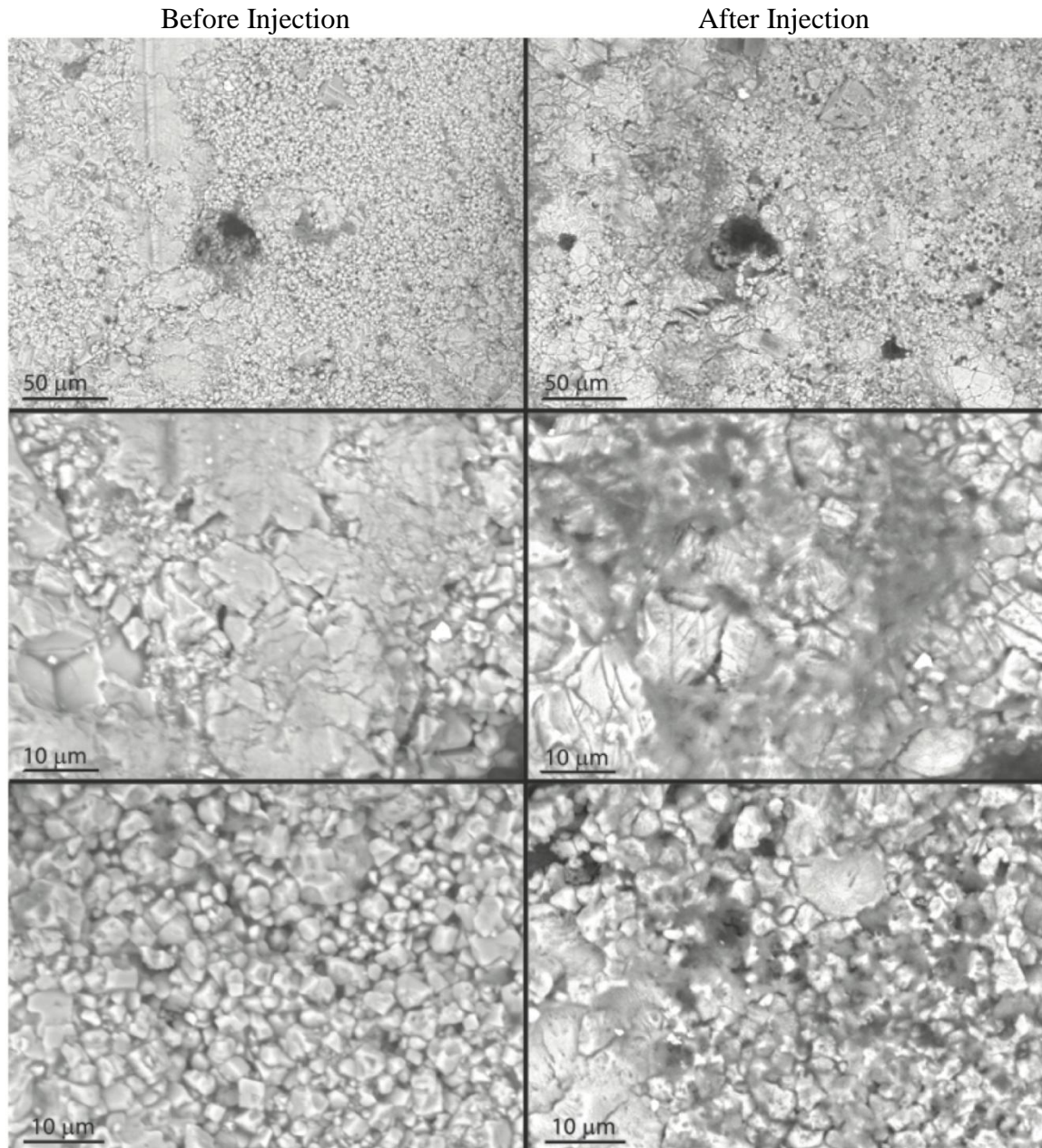


Figure 4: Time-lapse SEM images monitoring the changes in microstructure upon injection of a CO<sub>2</sub>-rich fluid in sample K. Initial microstructure at different magnifications is shown on the left panels and the same spots imaged after dissolution are shown on the right panels. K is a packstone (Dunham's classification) with few euhedral, subhedral, sometimes anhedral micritic zones and a high amount of dense and compact, sometimes coalescent cement.

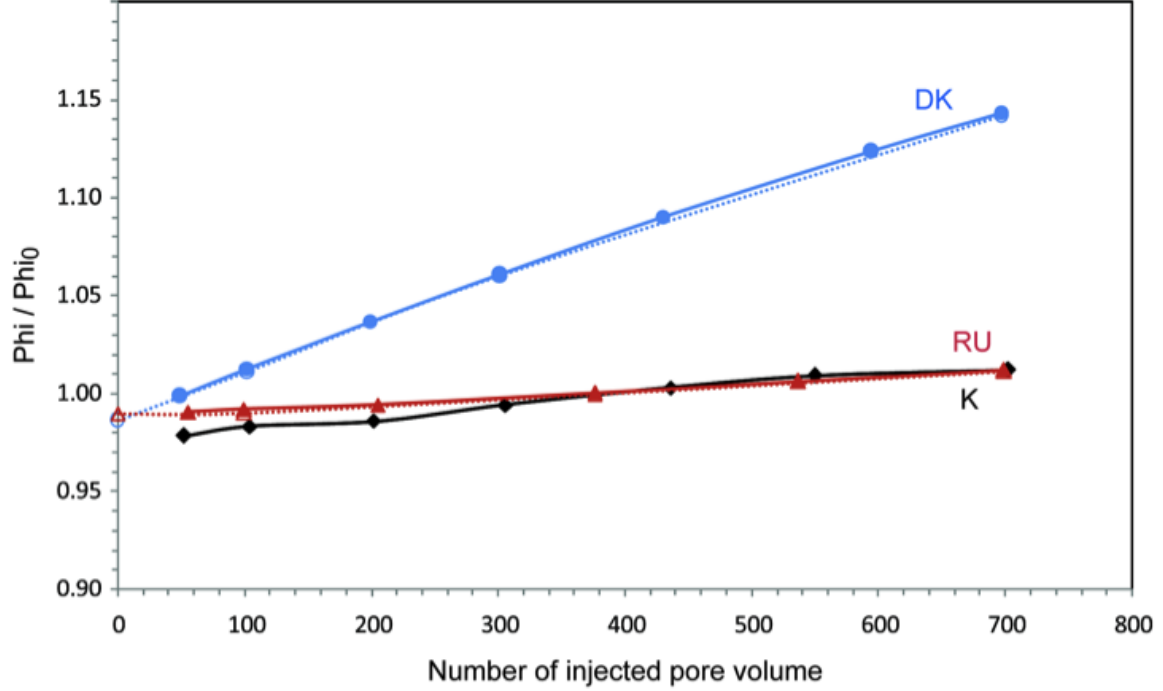


Figure 5: Change in total porosity as a function of injected pore volumes of fluid for all three samples. The variation in total porosity results from two competing and interdependent processes: chemical dissolution of calcite causing porosity increase and mechanical compaction under pressure causing porosity decrease.

### Estimation of reactive surface area during limestone dissolution

Reactive surface area is an important parameter because it influences the reactivity of many geological systems. It can be defined as the fraction of the geometrical surface area in contact with the saturating fluid and chemically active (chemical reactions occur only at selected sites on the minerals). Consequently, reactive surface area is not a parameter we can directly measure, and it is often used as a fitting parameter in many reactive transport simulators (Brosse et al., 2004). However, by using the chemistry of the output fluid and by making a number of hypotheses, it is possible to estimate an order of magnitude and to evaluate its variation with time. In the case of the dissolution of calcite, it is commonly assumed that the dissolution rate is (Lasaga and Kirkpatrick, 1981):

$$r = S_r \cdot k_c \cdot (1 - \Omega)$$

where  $r$  is the dissolution rate in mol/s,  $S_r$  the reactive surface area in  $m^2$ ,  $k_c$  the overall kinetic dissolution rate in  $mol/m^2/s$ , which depends on the pH of the solution and partial pressure of  $CO_2$ , and  $\Omega$  the calcite saturation index. Far from equilibrium and in absence of inhibitor species,  $k_c$  is given by (Plummer et al., 1978):

$$k_c = k_1 a_{H^+} + k_2 a_{H_2CO_3} + k_3$$

where  $k_1$ ,  $k_2$  and  $k_3$  are some kinetics rate constants and  $a_i$  the chemical activities. In a flow-through experiment, such as ours, the rate of dissolution can be also expressed by:

$$r = a_{Ca^{2+}} \cdot Q$$

where  $Q$  is the flow rate of the injected fluid. Consequently, the reactive surface area can be expressed as:

$$S_r = \frac{k_c \cdot (1 - \Omega)}{a_{Ca^{2+}} \cdot Q}$$

We have applied this to an experiment performed by Vialle (2008). It consisted in injecting a CO<sub>2</sub>-rich fluid in a limestone from Saint Maximin (France) under room pressure and temperature conditions and at a flow rate of 10mL/min. pH and Ca<sup>2+</sup> concentrations were continuously monitored and allowed the calculation of  $\Omega$  and  $k_c$ . By taking the average over the third injection, for example, and by assuming that the values measured at the outlet were the same through the entire rock (i.e., the flow rate of the injected fluid is slow enough to consider the reaction of dissolution instantaneous), a value of 36.4 m<sup>-1</sup> was obtained for  $S_r$ .

Several remarks can be made:

1. This value of reactive surface area, derived using the method above, is two orders of magnitude smaller than the geometrical surface area obtained by erosion-dilatation (4.69 10<sup>4</sup> m<sup>-1</sup>). This means that the surface areas measured (by gas adsorption like BET, by vertical scanning interferometry, atomic force microscopy, laser confocal microscopy or X-rays tomography) or geometrically constructed are not relevant for the reactivity of the rock.
2. This difference of two orders of magnitude is consistent with the experimental and computational work of Noiriél et al. (2010) regarding the dissolution of a limestone: while simulating (with the reaction-transport numerical code HYTEC) the chemistry of the output fluid, they were obliged to adjust the reactive surface areas by a value 18 to 480 times smaller (they differentiated micrite and sparite) than the one they obtained by 3D X-rays microtomography images analyses.

### **Numerical Simulation of Flow in the Slip Regime**

We are in the early states of developing tools for numerically simulating the chemical-mechanical effects that we are observing in the lab. Lattice Boltzmann methods (LBM) are a relatively new, efficient, and simple to implement method for simulating a variety of flow processes, i.e. single and multi-phase fluid flow, in any arbitrary geometry (McNamara and Zanetti, 1998). The Lattice Boltzmann equation has been shown to recover the continuum Navier-Stokes equations via Chapman-Enskog expansion (Chapman and Cowling, 1960) and accurately reproduces laboratory measured permeability values for clean sands (Keehm, 2003). In order to recover the continuum Navier-Stokes solutions, a no-slip (zero velocity) boundary condition is implemented at

fluid-solid boundaries; however, in simulations of gas flow, as the pore-throat width approaches the mean free path of the gas, molecule-wall collisions occur with increasing frequency and the fluid is no longer in thermodynamic equilibrium, and subsequently, the assumption of continuity is invalid (Knudsen, M., 1934). The Knudsen number – the ratio of mean free path ( $\lambda$ ) to channel width ( $L$ ) – defines different flow regimes which must be considered if the flow of gases is to be correctly simulated. A Knudsen number less than  $\sim 0.001$  is sufficient for continuity to hold, but for values between  $\sim 0.001$  and  $\sim 0.1$  (slip regime) gas slip across surfaces must be accounted for (Nie, et al., 2002). Non-negligible slip velocity across surfaces invalidates the no-slip boundary condition; as a result, a boundary condition that incorporates Knudsen number-dependent slip velocity must be implemented.

A Maxwellian reflection kernel is derived in terms of Lattice Boltzmann parameters (Zhang, et al., 2005), in which a gas-surface interaction-dependent accommodation coefficient,  $\alpha$ , weights reflections between purely diffusive reflections ( $\alpha = 1.0$ ) and purely specular reflections ( $\alpha = 0$ ) (Maxwell, 1879). The effect of changing the boundary condition is quantified by simulating flow profiles for CO<sub>2</sub> and quartz (a constitutive mineral in tight shale rocks) in a 2D pipe for Knudsen numbers in the slip regime ( $Kn = 0.01, 0.1$ ). The accommodation coefficient for CO<sub>2</sub> and quartz is 0.45 at 300K (Krylov, 1994) and the mean free path is given by

$$\lambda = \frac{k_B \cdot T}{\sqrt{2\pi P d^2}}$$

where  $k_B$  is the Boltzmann constant,  $T$  is the temperature,  $P$  is the pressure, and  $d$  is the molecular diameter. The onset of slip ( $Kn \sim 0.001$ ) for CO<sub>2</sub> ( $d = 0.407\text{nm}$  – [Hirschfelder, et al., 1954]) at sub-critical values,  $T = 300\text{K}$ ,  $P = 1\text{MPa}$ , occurs in pore-throats of  $5.628\mu\text{m}$ ; similarly,  $Kn = 0.01, 0.1$  correspond to pore-throat thicknesses of  $562.8\text{nm}$  and  $56.28\text{nm}$  respectively. The profiles of flow, non-dimensionalized by mean velocity, across the channel (Figure 6) show that traditional no-slip boundary conditions severely fail to reproduce Kn-dependent flow profiles. The average misfit (mean of percent error curve) is 19.6% for  $Kn = 0.01$  and 209.2% for  $Kn = 0.1$ ; subsequently, in rocks with nanometer-scale pore-throats traditional the no-slip boundary condition must be replaced with a slip boundary condition such as that presented in Zhang et al. 2005. Reformulation of this boundary condition to arbitrary geometries will enable the derivation of physically-realistic flow solutions for digital samples of real rocks, and is the subject of future work.

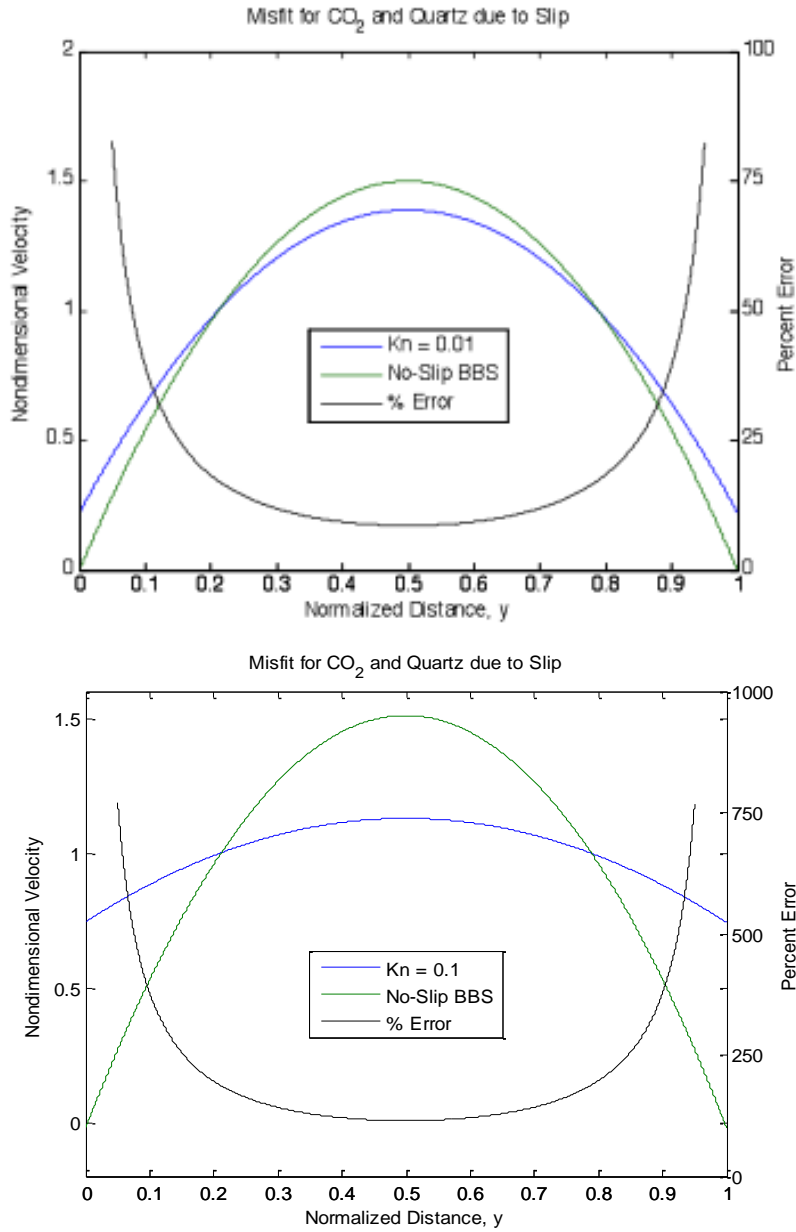


Figure 6: Flow profiles - no-slip in blue, slip in green - and percent error (black) curves for (top)  $Kn = 0.01$  and (bottom)  $Kn = 0.1$ . Percent error close to walls is not plotted as it trends to infinity since the no-slip velocity is exactly zero at the walls.

## References

- Brosse, E., Magnier, C., Vincent, B., 2004, Modelling fluid–rock interaction induced by the percolation of CO<sub>2</sub>-enriched solutions in core samples: the role of reactive surface area. *Oil Gas Sci. Technol.* 60 (2), 287–306.
- Chapman, S., Cowling, T.G., 1960, *The Mathematical Theory of Non-Uniform Gases*, Cambridge University Press
- Hirschfelder, J., Curtiss, C.F., Bird, R.B., 1954, *Molecular Theory of Gases and Liquids*, Wiley, New York
- Kehm, Y., 2003, Ph.D. thesis, Stanford University
- Knudsen, M., 1934, *The kinetic theory of gases*, Methuen and Co. Ltd., London
- Krylov, O.V., Shub, B.R., 1994, *Nonequilibrium processes in catalysis*, CRC Press, Boca Raton
- Lasaga, A.C., Kirkpatrick, R.J. (Eds.), 1981, Kinetics of Geochemical Processes. . Reviews in Mineralogy, vol. 8. Mineralogical Society of America, Washington DC. 398 pp.
- Maxwell, J.C., 1879, *On Stresses in Rarified Gases Arising from Inequalities of Temperature*, *Phil. Trans. R. Soc. Lond.*, 170, 231-256
- McNamara, G.R., Zanetti, G., 1998, *Use of the Boltzmann equation to simulate lattice-gas automata*, *Phys. Rev. Lett.*, 61, 2332
- Nie, X., Doolen, G.D., Chen, S., 2002. *Lattice-Boltzmann Simulations of Fluid Flows in MEMS*, *J. Stat. Phys.*, 107, 1-2
- Noiriel C., Luquot L., Madé B., Raimbault L., Gouze P. and van der Lee J. (2009) Changes in reactive surface area during limestone dissolution: an experimental and modelling study, *Chemical Geology*, 265(1-2), 160-170.
- Plummer L.N, Wigley T.M.L. and Parkhurst D.L., 1978, The kinetics of calcite dissolution in CO<sub>2</sub>-water systems at 5 to 60°C and 0.0 to 1.0 atm CO<sub>2</sub>, *American Journal of Science*, 278, 179-216;
- Vialle, S. (2008), Etude expérimentale des effets de la dissolution (ou de la précipitation) de minéraux sur les propriétés de transport des roches, PhD Thesis, Institut de Physique du Globe de Paris, University Denis Diderot, Paris, France, 262p.
- Zhang, Y., Qin, R., and Emerson, D.R., 2005. *Lattice Boltzmann simulation of rarefied gas flows in microchannels*, *Phys. Rev. E*, 71, 04

## **Progress**

Sequestration of CO<sub>2</sub> in geological formations is one of the carbon-management technologies having the potential to substantially reduce greenhouse gas emissions while achieving energy sustainability. To translate such potential into concrete development outcomes, realized benefits, and policy, common concerns (i.e. pore pressures reactivating faults or fractures, risk of leakages, and loss of storage capacity) need to be dispelled. These concerns are thus intimately associated with our ability to use geophysical techniques to monitor chemical processes and their effects on the rock properties. Exploring the links between geophysical observables, rock physical properties, and geochemical induced long-term changes upon CO<sub>2</sub> sequestration and introducing them into standard monitoring programs are necessary steps to go towards quantitative predictions of pore pressure, saturation, and storage capacity.

This project is on track to meet the overall objectives. The laboratory techniques for ultrasonic monitoring of rock changes associated with CO<sub>2</sub> injection have been refined and demonstrated. Significant injection-related changes in elastic moduli and increases in porosity and permeability have been observed, which provide the impetus for developing an improved rock physics model for CO<sub>2</sub> monitoring. The subcontract is now in place with our team members at Rice University. They are beginning their measurements and analysis of reaction rates, which will help to better understand the elastic, porosity, and permeability changes that have been observed.

## **Future Plans**

Laboratory experiments will continue on monitoring the changes in rock elastic and transport properties during injection of CO<sub>2</sub>-brine mixtures. One new aspect will be to understand the reactions under various effective stresses, which cause the opening and closing of cracks and changes in contact stress. Numerical simulations of reactive flow in the pore space will begin. Laboratory experiments on specific chemical reaction rates will be made by team members at Rice University.

## **Contacts**

Gary Mavko: [mavko@stanford.edu](mailto:mavko@stanford.edu)

Sally Benson: [smbenson@stanford.edu](mailto:smbenson@stanford.edu)

Tiziana Vanorio: [tvorio@stanford.edu](mailto:tvorio@stanford.edu)

Stephanie Vialle: [svialle@stanford.edu](mailto:svialle@stanford.edu)

Andreas Luttge: [aluttge@rice.edu](mailto:aluttge@rice.edu)

Rolf Arvidson: [rolf.s.arvidson@rice.edu](mailto:rolf.s.arvidson@rice.edu)